

Strength of Stiffened 2024-T3 Aluminum Panels with Multiple Site Damage

B. L. Smith,* A. L. Hijazi,† A. K. M. Haque,‡ and R. Y. Myose‡
Wichita State University, Wichita, Kansas 67260-0044

Two modified linkup models were developed for determining the critical stress based on linkup (ligament failure) of 2024-T3 aluminum panels with multiple site damage. These models were developed for use with standard Military Handbook for Metallic Materials and Elements for Aerospace Vehicle Structures (MIL-HDBK-5G) yield strength values. For this investigation, ligament failure stresses predicted by these models are compared with test stresses determined from a variety of stiffened panels including single-bay panels with the lead crack centered between stiffeners and two-bay panels with the lead crack centered beneath a severed stiffener. The stresses predicted by the modified linkup models correlate well with the test data. The results of this investigation should add to the understanding of the extent to which nonlinear behavior can be modeled with simplified engineering models.

Nomenclature

a	= lead crack half-length
a_n	= nominal lead crack half-length
c	= multiple site damage (MSD) crack length
D	= hole diameter
F_{col}	= collapse stress
ℓ	= half-length for MSD crack and hole, $c + D/2$
L	= ligament length
t	= panel thickness
t_s	= stiffener thickness
W	= panel width
W_s	= stiffener width
β_a	= correction to stress intensity of the lead crack, $\beta_w \beta_{a/\ell} \beta_s$
$\beta_{a/\ell}$	= correction to stress intensity of the lead crack for the effect of the adjacent MSD crack
β_b	= correction to stress intensity of the adjacent MSD crack for the effect of an open hole
β_ℓ	= correction to stress intensity of the adjacent MSD crack, $\beta_{\ell/a} \beta_b \sqrt{c/\ell}$
$\beta_{\ell/a}$	= correction to stress intensity of the adjacent MSD crack for the effect of the lead crack
β_s	= stiffener correction to stress intensity of the lead crack
β_w	= finite width correction to the stress intensity of the lead crack, $\sqrt{[\sec(\pi a/w)]}$
σ_c	= critical stress for ligament failure based on modified linkup
σ_{lu}	= critical stress for ligament failure based on linkup (coalescence of plastic zones), $\sigma_{ys} \sqrt{[2L/(a\beta_a^2 + \ell\beta_\ell^2)]}$
σ_{test}	= critical stress for ligament failure obtained from testing
σ_{ys}	= yield strength

Introduction

FATIGUE damage in the form of small-scale cracking, commonly referred to as multiple site damage (MSD), accumulates in aging aircraft. Skin panels with major (lead) cracks exhibit a loss in strength. However, panels with MSD in addition to major cracks may exhibit a further loss in strength, especially panels of ductile materials such as 2024-T3 aluminum. Until recently the additional loss in strength caused by MSD was often ignored. In an

attempt to explain this phenomenon, Swift¹ described an analytical model commonly referred to as the linkup model or plastic-zone-touch model. Many analytical models describing phenomenon such as this are unwieldy and impractical for engineering application. However, the linkup model is simple to use and is practical for engineering practice. The linkup model clearly shows an additional loss of strength from MSD, but it does not accurately predict the magnitude of the loss for many geometric configurations.

A schematic of a panel with multiple site damage is shown in Fig. 1. It has a central lead crack of length $2a$ and collinear MSD cracks emerging from the adjacent holes. Although this diagram is of a flat unstiffened panel with open holes, the linkup model is formulated so that it may be used for panels with more complex configurations, as long as the stress intensities of the lead crack tip and the adjacent MSD crack tip can be determined. According to the linkup phenomenon, the ligament L is assumed to fail when the plastic zone of the lead crack touches the plastic zone of the adjacent MSD crack. A value of the remote stress σ that produces ligament failure from linkup (coalescence of plastic zones), and subsequent crack extension, is given as follows¹:

$$\sigma_{lu} = \sigma_{ys} \sqrt{\frac{2L}{a\beta_a^2 + \ell\beta_\ell^2}} \quad (1)$$

where σ_{ys} is the yield strength of the panel material. Equation (1) is based on the Irwin representation of plastic zone size.

Several modifications of the linkup model have been developed and reported in the literature, one by Broek² and more recently by Ingram et al.³ of Lockheed Martin Corporation (LMC). These models are, respectively,

$$\sigma_c = \left\{ 0.5 + 0.9 \left[\frac{1}{1 + L/a} \right] \right\} F_{col} \sqrt{\frac{L}{a\beta_a^2 + \ell\beta_\ell^2}} \quad (2)$$

$$\sigma_c = \left[1.83 - \exp\left(-0.57 \frac{a}{L}\right) \right] \sigma_{ys} \sqrt{\frac{L}{a\beta_a^2 + \ell\beta_\ell^2}} \quad (3)$$

The Broek model² [Eq. (2)] was developed from an empirical analysis based on the test data from 20-in.-wide panels tested at Foster-Miller, Inc.⁴ The collapse stress F_{col} was determined by Broek² as 37.5 ksi for 2024-T3 material. The Broek model is not a direct function of yield strength. The test database for this model included only clad material, a single panel thickness of 0.04 in., and loading in the long transverse (LT) grain direction (load perpendicular to grain). The LMC model [Eq. (3)] was developed from an empirical analysis based on test data from the Foster-Miller panels, from 90-in.-wide panels tested by the National Institute of Standards

Received 7 July 2000; revision received 14 September 2000; accepted for publication 21 September 2000. Copyright © 2001 by the authors. Published by the American Institute of Aeronautics and Astronautics, Inc., with permission.

*Professor, Department of Aerospace Engineering. Member AIAA.

†Graduate Research Assistant, Department of Aerospace Engineering.

‡Associate Professor, Department of Aerospace Engineering. Associate Fellow AIAA.

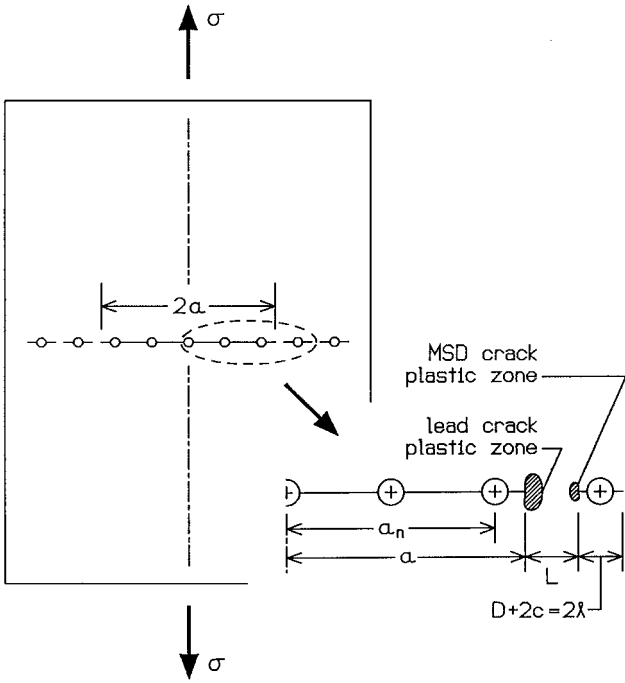


Fig. 1 Schematic diagram of panel with MSD.

and Technology (NIST),⁵ and from 24-in.-wide panels tested at Wichita State University (WSU).⁶ The LMC model was also based on yield strength values for the panels reported by Foster-Miller, NIST, and WSU, rather than Military Handbook for Metallic Materials and Elements for Aerospace Vehicle Structures (MIL-HDBK-5G) values. In another investigation, Kuang and Chen⁷ presented an analysis of ligament failure from MSD based on coalescence of plastic zones determined from the narrow-strip Dugdale model. In that investigation, cases were examined resulting in an average absolute difference of 9.67% between analytical and measured stresses.

Two modified linkup models were developed by Smith et al.⁶ from an empirical analysis based on test data from 40 different panel configurations. These panels were flat, unstiffened panels without fastener loads. At Foster-Miller (see Ref. 4) 9 were tested, at NIST (see Ref. 5) 9 were tested, and at WSU (see Ref. 6) 22 were tested. Excellent results were obtained from these two modified linkup models. These models, referred to as WSU linkup models 2 and 3 (WSU2 and WSU3), are easy to use and still give accurate results for a large range of parameters including panel thickness and width, lead crack length, MSD crack length, grain direction, and ligament length. WSU2 and WSU3 models are, respectively,

$$\sigma_c = \frac{\sigma_{ys} \sqrt{2L / (a\beta_a^2 + \ell\beta_\ell^2)}}{C_1[\ln(L)] + (C_2 + 1)} = \frac{\sigma_{lu}}{C_1[\ln(L)] + (C_2 + 1)} \quad (4)$$

$$\sigma_c = \frac{\sigma_{ys} \sqrt{2L / (a\beta_a^2 + \ell\beta_\ell^2)}}{C_3[\ln(a/L)] + (C_4 + 1)} = \frac{\sigma_{lu}}{C_3[\ln(a/L)] + (C_4 + 1)} \quad (5)$$

The basic difference between these two modified linkup models is that Eq. (5) model is a nondimensionalized version of the Eq. (4) model. Both were developed through a similar empirical analysis. The stresses given by Eqs. (1–5) are in kilopounds per square inch, and the ligament lengths and half-crack lengths are in inches. The analytical models given in Eqs. (4) and (5) were developed for use with A-basis or B-basis yield strength values from MIL-HDBK-5G because these are the values of yield strength that practicing engineers in the aerospace industry would most likely use. When A-basis yield strength values are used in Eq. (4), the coefficients are $C_1 = 0.3065$ and $C_2 = 0.3123$. For the B-basis yield strength values, the coefficients are $C_1 = 0.3054$ and $C_2 = 0.3502$. When A-basis values are used in Eq. (5), the coefficients are $C_3 = -0.1806$ and $C_4 = 0.4791$, and for the B-basis development, the coefficients are $C_3 = -0.1813$

and $C_4 = 0.5193$. An earlier paper⁸ had slightly different coefficients because of several incorrect values of yield strength taken from MIL-HDBK-5G. The coefficients were corrected in Ref. 6 as well as this paper even though the results are only slightly different. The complete details of the development of Eqs. (4) and (5) are given in Ref. 6 and are not repeated here. Also, in Ref. 6, the critical stresses were determined from Eqs. (1–6) and compared for 40 different cases.

The primary purpose of the work described herein was to validate the analytical models given in Eqs. (4) and (5) with test data from stiffened panels. Two different basic stiffened panel configurations have been investigated. One configuration is a single-bay stiffened panel with MSD at open holes in addition to a lead crack centered between stiffeners (Fig. 2). The other configuration is a two-bay stiffened panel with MSD at open holes in addition to a lead crack centered below a simulated broken central stiffener (Fig. 3). The

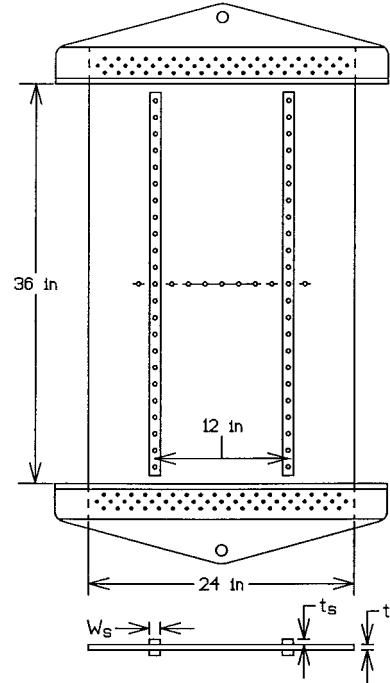


Fig. 2 Single-bay stiffened panel.

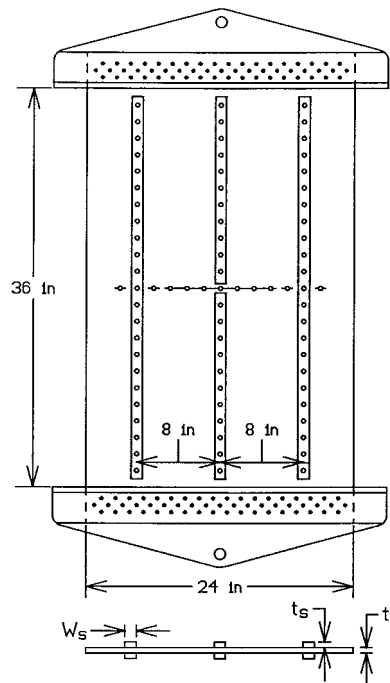


Fig. 3 Two-bay stiffened panel.

results of this investigation should add to the understanding of the extent to which nonlinear behavior can be described through the use of simplified engineering models.

Geometric Corrections to Stress Intensity

The corrections to stress intensity of the lead crack and the adjacent MSD crack are

$$\beta_a = \beta_w \beta_{a/\ell} \beta_s \tag{6}$$

$$\beta_\ell = \beta_{\ell/a} \beta_b \sqrt{c/\ell} \tag{7}$$

where $\beta_{a/\ell}$ and $\beta_{\ell/a}$ represent the effects of collinear adjacent crack tips on each other⁹ and β_w is the finite width correction given by the square root of $\sec(\pi a/w)$. The term β_b accounts for the effect of the hole on the MSD crack tip¹⁰ given by the following equation:

$$\beta_b = 1 - \frac{0.15}{1 + 2c/D} + \frac{3.46}{(1 + 2c/D)^2} - \frac{4.47}{(1 + 2c/D)^3} + \frac{3.52}{(1 + 2c/D)^4} \tag{8}$$

The term β_s is the correction to the stress intensity of the lead crack for the effect of stiffeners. For the case of the single-bay panel with the lead crack centered between the two stiffeners as shown in Fig. 2, the quantity β_s was determined from the work of Poe¹¹ and verified by the use of the FRANC2D/L software.¹² The FRANC2D/L software was also used to determine the effect of the stiffeners on the adjacent MSD crack. However, it was found to have little effect on the resulting linkup stress because the $a(\beta_a)^2$ term is very dominant over the $\ell(\beta_\ell)^2$ term. Subsequently, the stiffener effects on the adjacent MSD cracks were not included for either of the stiffened panel models investigated. For the case of the two-bay panel with the severed stiffener shown in Fig. 3, β_s was determined from a special

computer program developed at Cessna Aircraft Corporation based on the methodology and procedures developed by Swift.¹³

Experimental Setup and Test Data

A servo-hydraulic testing machine was used to determine the linkup stress for 21 single-bay panel configurations and for 15 two-bay panel configurations. Figure 2 shows the plan view and cross-sectional view of a single bay panel, whereas Fig. 3 shows the two-bay panel. The lead crack in the single-bay panel is centered between stiffeners, whereas the lead crack in the two-bay panels is centered beneath a simulated severed stiffener. In both cases, MSD cracks emerge from both sides of open holes adjacent to the lead crack. All of the 2024-T3 clad panels are 24 in. wide, and all but one is 0.063 in. thick. The open holes along the crack line are 0.25 in. in diameter with a pitch of 1.0 in.

The bay width in the single-bay panels is 12 in. and it is 8 in. in the two-bay panels. The stiffeners are rectangular in cross section and are on both sides of the panel. Stiffeners are fastened to the panels with 0.25-in.-diam steel bolts with a pitch of 1.0 in. Midspan fixtures, not shown in the figures, were used to prevent buckling along the crack line, and heavy fixtures were used at each end to help distribute the load evenly across the width. Panel and stiffener details are given in Table 1, where the first 21 panels are the single-bay panels and the last 15 (panel numbers 22–36) are the two-bay panels. The remote stresses producing linkup, σ_{test} , are given in both Tables 2 and 3. These stresses may be converted into loads by multiplying them by the appropriate gross cross-sectional areas (total area of panel plus stiffeners). Stroke control was used at a rate of 0.01 in./min.

The manufactured MSD cracks were produced either by electrodischarge-machine (EDM) or by a jeweler’s saw. The EDM

Table 1 Panel configuration

Panel no.	<i>t</i> , in.	Crack type	<i>a</i> , in.	<i>c</i> , in.	<i>L</i> , in.	<i>W_S</i> , in.	<i>t_S</i> , in.	Load direction
1	0.063	EDM	4.675	0.05	0.15	1.05	0.31	LT
2	0.063	EDM	4.575	0.05	0.25	1.05	0.31	LT
3	0.063	EDM	4.475	0.05	0.35	1.05	0.31	LT
4	0.063	EDM	4.275	0.15	0.45	1.05	0.31	LT
5	0.063	EDM	4.225	0.10	0.55	1.05	0.31	LT
6	0.063	EDM	4.175	0.05	0.65	1.05	0.31	LT
7	0.063	EDM	5.675	0.05	0.15	1.05	0.31	LT
8	0.063	EDM	5.575	0.05	0.25	1.05	0.31	LT
9	0.063	EDM	5.475	0.05	0.35	1.05	0.31	LT
10	0.063	EDM	5.275	0.15	0.45	1.05	0.31	LT
11	0.063	EDM	5.225	0.10	0.55	1.05	0.31	LT
12	0.063	EDM	5.175	0.05	0.65	1.05	0.31	LT
13	0.063	Saw	4.475	0.05	0.35	1.00	0.50	L
14	0.063	Saw	4.275	0.15	0.45	0.94	0.50	L
15	0.063	Saw	4.225	0.10	0.55	0.94	0.50	L
16	0.063	Saw	4.175	0.05	0.65	0.94	0.50	L
17	0.063	Saw	5.675	0.05	0.15	1.00	0.50	L
18	0.063	Saw	5.275	0.15	0.45	0.94	0.50	L
19	0.063	Saw	5.225	0.10	0.55	1.00	0.50	L
20	0.063	Saw	5.175	0.05	0.65	1.00	0.50	L
21	0.040	Saw	3.225	0.10	0.55	1.05	0.31	L
22	0.063	EDM	4.225	0.10	0.55	1.05	0.31	LT
23	0.063	EDM	4.275	0.15	0.45	1.05	0.31	LT
24	0.063	EDM	4.325	0.20	0.35	1.05	0.31	LT
25	0.063	EDM	5.225	0.10	0.55	1.05	0.31	LT
26	0.063	Saw	5.275	0.15	0.45	1.05	0.31	LT
27	0.063	EDM	5.325	0.20	0.35	1.05	0.31	LT
28	0.063	EDM	6.225	0.10	0.55	1.05	0.31	LT
29	0.063	EDM	6.275	0.15	0.45	1.05	0.31	LT
30	0.063	Saw	6.325	0.20	0.35	1.05	0.31	LT
31	0.063	EDM	7.225	0.10	0.55	1.05	0.31	LT
32	0.063	EDM	7.275	0.15	0.45	1.05	0.31	LT
33	0.063	EDM	7.325	0.20	0.35	1.05	0.31	LT
34	0.063	Saw	4.225	0.10	0.55	1.05	0.31	L
35	0.063	Saw	5.225	0.10	0.55	1.05	0.31	L
36	0.063	Saw	6.225	0.10	0.55	1.05	0.31	L

Table 2 Stresses based on A-basis yield strengths

Panel no.	σ_{ys}					Linkup % error	WSU2 % error	WSU3 % error
	A-basis, ksi	σ_{test} , ksi	σ_{lu} , ksi	$\sigma_{c,WSU2}$, ksi	$\sigma_{c,WSU3}$, ksi			
1	40.0	10.60	7.91	10.82	9.22	25.43	2.04	13.08
2	40.0	12.61	11.18	12.60	11.72	11.33	0.08	7.07
3	40.0	14.49	13.91	14.05	13.66	4.00	3.08	5.78
4	40.0	13.84	15.64	14.65	14.58	12.99	5.84	5.35
5	40.0	16.05	18.14	16.06	16.33	13.02	0.10	1.74
6	40.0	17.72	20.58	17.44	18.00	16.14	1.60	1.59
7	40.0	10.83	8.02	10.97	9.75	25.96	1.31	10.03
8	40.0	12.86	11.25	12.68	12.25	12.56	1.46	4.79
9	40.0	14.08	13.80	13.94	14.05	1.94	1.00	0.19
10	40.0	13.96	15.06	14.11	14.56	7.90	1.07	4.30
11	40.0	16.34	17.36	15.38	16.19	6.28	5.87	0.91
12	40.0	18.54	19.64	16.64	17.78	5.92	10.26	4.10
13	45.0	15.53	15.97	16.12	15.67	2.83	3.81	0.93
14	45.0	15.75	17.84	16.71	16.63	13.28	6.11	5.62
15	45.0	17.39	20.70	18.33	18.63	19.02	5.41	7.14
16	45.0	18.97	23.53	19.93	20.58	24.03	5.09	8.49
17	45.0	11.82	9.44	12.92	11.47	20.16	9.24	2.98
18	45.0	16.54	17.36	16.27	16.78	5.00	1.64	1.49
19	45.0	17.45	20.09	17.79	18.73	15.11	1.95	7.32
20	45.0	20.21	22.71	19.24	20.56	12.33	4.83	1.71
21	45.0	18.96	23.08	20.44	19.90	21.71	7.79	4.95
22	40.0	11.68	13.89	12.30	12.51	18.93	5.33	7.06
23	40.0	10.28	12.10	11.33	11.28	17.74	10.29	9.78
24	40.0	8.51	10.14	10.24	9.89	19.21	20.35	16.30
25	40.0	11.00	12.60	11.16	11.75	14.56	1.47	6.82
26	40.0	9.84	10.99	10.30	10.62	11.75	4.68	8.02
27	40.0	8.23	9.22	9.31	9.34	12.08	13.15	13.50
28	40.0	10.48	11.58	10.26	11.13	10.53	2.10	6.19
29	40.0	9.27	10.10	9.47	10.07	9.04	2.14	8.69
30	40.0	7.94	8.48	8.56	8.87	6.89	7.91	11.77
31	40.0	9.97	10.96	9.70	10.81	9.90	2.66	8.38
32	40.0	8.84	9.59	8.98	9.82	8.43	1.57	11.04
33	40.0	7.52	8.07	8.15	8.68	7.24	8.26	15.33
34	45.0	14.07	15.63	13.84	14.07	11.10	1.60	0.01
35	45.0	12.22	14.18	12.56	13.22	16.08	2.81	8.23
36	45.0	11.94	13.03	11.54	12.52	9.12	3.36	4.83

Table 3 Stresses based on B-basis yield strengths

Panel no.	σ_{sys} , ksi	σ_{test} , ksi	σ_{lu} , ksi	$\sigma_{c, \text{WSU2}}$, ksi	$\sigma_{c, \text{WSU3}}$, ksi	Linkup % error	WSU2 % error	WSU3 % error
1	42.0	10.60	8.30	10.77	9.27	21.70	1.58	12.59
2	42.0	12.61	11.74	12.67	11.83	6.90	0.45	6.17
3	42.0	14.49	14.61	14.19	13.82	0.80	2.10	4.66
4	42.0	13.84	16.42	14.84	14.78	18.64	7.24	6.78
5	42.0	16.05	19.04	16.31	16.57	18.67	1.63	3.22
6	42.0	17.72	21.61	17.73	18.28	21.95	0.07	3.16
7	42.0	10.83	8.42	10.92	9.79	22.26	0.85	9.67
8	42.0	12.86	11.81	12.74	12.35	8.18	0.94	4.00
9	42.0	14.08	14.49	14.08	14.20	2.96	0.01	0.87
10	42.0	13.96	15.81	14.29	14.74	13.30	2.41	5.59
11	42.0	16.34	18.23	15.62	16.41	11.59	4.43	0.43
12	42.0	18.54	20.62	16.92	18.04	11.21	8.74	2.71
13	47.0	15.53	16.67	16.20	15.77	7.40	4.32	1.58
14	47.0	15.75	18.63	16.84	16.77	18.32	6.94	6.48
15	47.0	17.39	21.62	18.52	18.81	24.31	6.46	8.13
16	47.0	18.97	24.57	20.16	20.79	29.54	6.30	9.59
17	47.0	11.82	9.86	12.79	11.46	16.61	8.18	3.11
18	47.0	16.54	18.14	16.39	16.90	9.67	0.87	2.20
19	47.0	17.45	20.98	17.97	18.88	20.22	2.96	8.20
20	47.0	20.21	23.72	19.46	20.75	17.32	3.73	2.63
21	47.0	18.96	24.11	20.64	20.11	27.12	8.87	6.05
22	42.0	11.68	14.59	12.49	12.69	24.88	6.95	8.62
23	42.0	10.28	12.70	11.48	11.43	23.63	11.74	11.26
24	42.0	8.51	10.65	10.34	10.01	25.17	21.58	17.70
25	42.0	11.00	13.24	11.34	11.91	20.29	3.02	8.26
26	42.0	9.84	11.54	10.43	10.76	17.34	6.06	9.36
27	42.0	8.23	9.68	9.40	9.44	17.68	14.30	14.73
28	42.0	10.48	12.16	10.42	11.27	16.06	0.60	7.52
29	42.0	9.27	10.61	9.59	10.19	14.49	3.49	9.92
30	42.0	7.94	8.91	8.65	8.96	12.24	9.01	12.85
31	42.0	9.97	11.50	9.85	10.93	15.39	1.17	9.65
32	42.0	8.84	10.07	9.10	9.92	13.85	2.91	12.20
33	42.0	7.52	8.47	8.23	8.75	12.60	9.37	16.33
34	47.0	14.07	16.32	13.98	14.20	16.03	0.62	0.93
35	47.0	12.22	14.81	12.68	13.33	21.24	3.83	9.11
36	47.0	11.94	13.61	11.66	12.61	13.97	2.39	5.58

cracks were produced with a 0.004-in.-diam wire resulting in actual crack widths of 0.005 in., whereas the cracks produced with the jeweler's saw were approximately 0.007 in. in width. When EDM cracks were used, it was only necessary to test one panel per configuration because of the consistency in results. However, when cracks were produced by a jeweler's saw, it was necessary to test several panels per configuration because the results were not as consistent. For those configurations where duplicate panels were tested, each test value given in Tables 2 and 3 represents the average value.

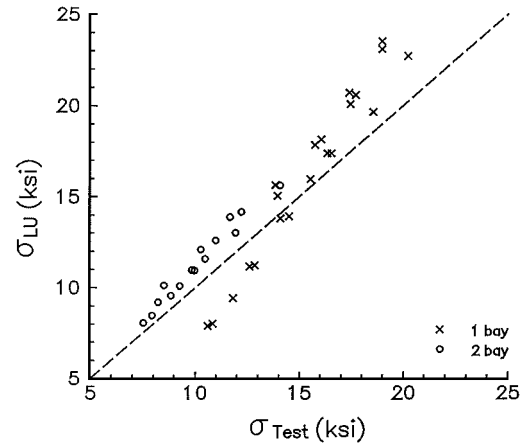
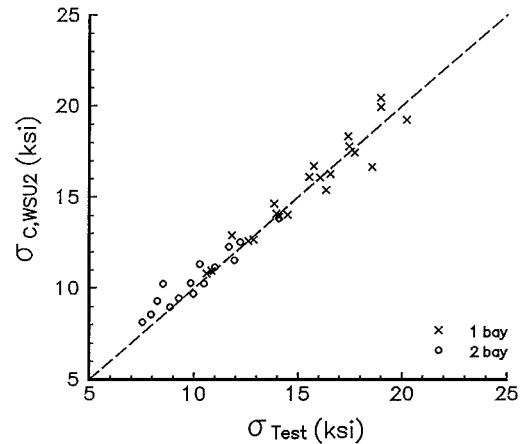
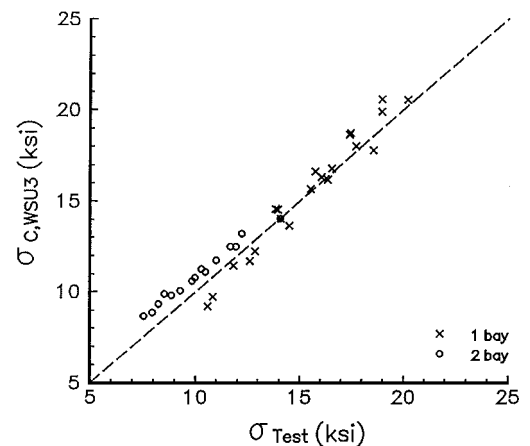
As noted in Ref. 6, there was some concern about the use of crack tips produced by EDM or saw cut for obtaining reliable results for residual strength tests, as compared with fatigue sharpened crack tips. Dawicke et al.¹⁴ showed a significant difference in the results between using these two types of crack tips. However, Heinemann¹⁵ and Seson¹⁶ concluded that narrow EDM slots, such as those used in this investigation, provided a suitable method for residual strength tests requiring consistent initial configurations.

Results

The remote stresses producing linkup determined from Eqs. (1), (4), and (5) and based on A-basis yield strength values are given in Table 2. Table 3 has the corresponding stresses for B-basis yield strength values. The first 21 panels are the one-bay panels with the lead crack centered between stiffeners, as shown in Fig. 2. The last 15 panels are the two-bay panels with the lead crack centered under a severed stiffener, as shown in Fig. 3. Tables 1 and 2 also give the errors between the analytical models and the test values. Error is defined as the absolute value of the percent difference between the test value and the analytical model. When using A-basis yield strength values, the average error between the stresses predicted by the linkup model of Eq. (1) and the test values for the 36 stiffened panels is 12.76%, whereas the error for the WSU2 and WSU3 mod-

els of Eqs. (4) and (5) are 4.65 and 6.54%, respectively. When using B-basis values, the error for the linkup model of Eq. (1) is 16.49%, whereas the errors for the WSU2 and WSU3 models are 4.89 and 7.27%, respectively.

Figures 4–9 provide graphic representations of these results. Figures 4–9 compare the test stresses with the stresses predicted by one of the analytical models. In Figs. 4–9, the ideal situation would be for all of the points to fall on the 45-deg line. An \times is used for the one-bay stiffened panels and a circle is used for the two-bay panels. It is apparent that the two modified linkup models give significantly better results than the original linkup model. For the configurations considered herein, given in Table 1, the critical

**Fig. 4** A-basis σ_{lu} vs σ_{test} .**Fig. 5** A-basis $\sigma_{c, \text{WSU2}}$ vs σ_{test} .**Fig. 6** A-basis $\sigma_{c, \text{WSU3}}$ vs σ_{test} .

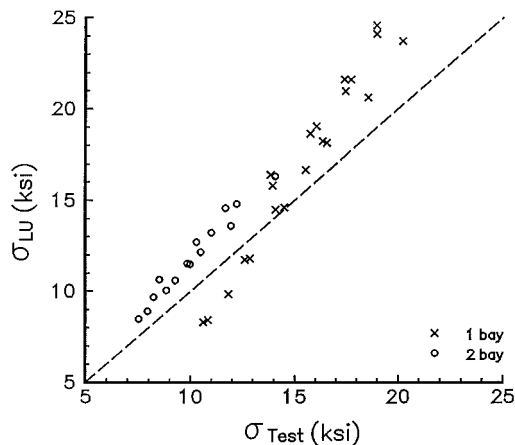


Fig. 7 B-basis σ_{Lu} vs σ_{test} .

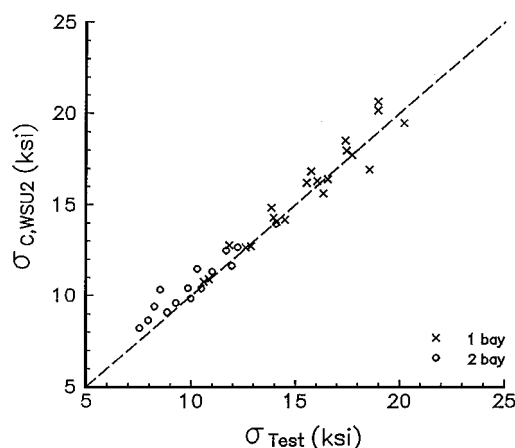


Fig. 8 B-basis $\sigma_{c,WSU2}$ vs σ_{test} .

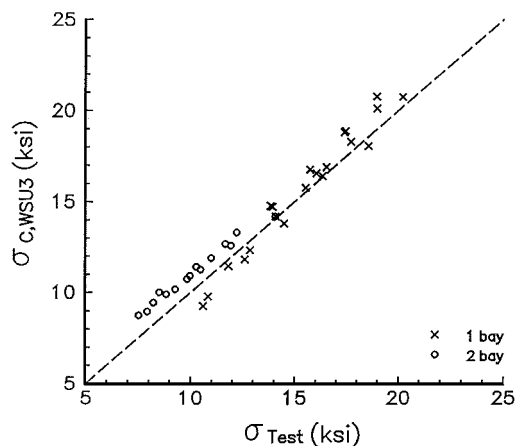


Fig. 9 B-basis $\sigma_{c,WSU3}$ vs σ_{test} .

stresses based on coalescence of plastic zones were lower than the critical stresses corresponding to yielding of the net section.

Conclusions

Two modified linkup models have been developed from test data for flat unstiffened open-hole panels. One of these is a nondimensionalized version of the other. Both are functions of yield strength and have been developed for use with A-basis or B-basis yield strength values. The results of both models have been compared with test data from 36 stiffened panels including 21 one-bay panels with different crack configurations and 15 two-bay panels with different crack configurations. Based on this comparison, the two

modified linkup models are significantly more accurate than the original linkup model. All of the 36 panels have the same overall dimensions, and all but one have the same thickness. However, lead crack lengths and MSD crack lengths vary over a wide range, some panels were loaded in the LT grain direction whereas others were loaded in the L direction, and panels were obtained from several different lots. These modified models were developed from a database containing both bare and clad 2024-T3 aluminum; however, the 36 stiffened panels tested in this project were clad.

The development of these modified linkup models was based on test data for a simple configuration (flat, unstiffened, open-hole panels). However, the results presented herein support the idea that they may be successfully used for panels with more complex configuration provided that stress intensity factors for the lead crack and the adjacent MSD crack can be determined. The results also indicate some success in representing nonlinear behavior with simplified engineering models.

Acknowledgments

This work was sponsored by the industry members of the Aircraft Design and Manufacturing Research Center of Wichita State University, Wichita, Kansas. The material for the aluminum panels was donated by Alcoa Aerospace Center, Hutchinson, Kansas. The electrodischarge-machine cracks were produced by the Materials Testing Laboratory of The Boeing Company, Wichita, Kansas. Their support is greatly appreciated.

References

- Swift, T., "Widespread Fatigue Damage Monitoring Issues and Concerns," *Proceedings of the 5th International Conf. on Structural Airworthiness of New and Aging Aircraft*, Hamburg, Germany, June 1993.
- Brock, D., "The Effects of Multi-Site Damage on the Arrest Capability of Aircraft Fuselage Structure," *Fracture Research*, Galena, OH, TR 9302, June 1993.
- Ingram, J. E., Kwon, Y. S., Duffie, K. J., and Irby, W. D. "Residual Strength Analysis of Skin Splices with Multiple Site Damage," NASA/CP-1999-208982, Sept. 1998.
- Thompson, D., Hoadley, D., and McHatton, J., "Load Tests of Flat and Curved Panels with Multiple Cracks," Foster-Miller, Inc., Waltham, MA, Sept. 1993.
- Fields, R., Low, S., III, Hame, D., and Froeche, T., "Fracture Testing of Large-Scale Thin-Sheet Aluminum Alloy," National Inst. of Standards and Technology, Rept. NISTIR 5661, Gaithersburg, MD, May 1995.
- Smith, B., Saville, P., Mouak, A., and Myose, R., "Strength of 2024-T3 Aluminum Panels with Multiple Site Damage," *Journal of Aircraft*, Vol. 37, No. 2, 2000, pp. 325–331.
- Kuang, J. H., and Chen, C. K., "The Failure of Ligaments Due to Multiple-Site Damage Using Interactions of Dugdale-Type Cracks," *Fatigue and Fracture of Engineering Materials and Structures*, Vol. 21, 1998, pp. 1147–1156.
- Smith, B., Hijazi, A., Haque, A. K. M., and Myose, R., "Modified Linkup Models for Determining the Strength of Stiffened Panels with Multiple Site Damage," *Proceedings of the 3rd Joint NASA/Federal Aviation Administration/Dept. of Defense Conf. on Aging Aircraft*, Sept. 1999.
- Rooke, D. P., and Cartwright, D. J., *Compendium of Stress Intensity Factors*, Her Majesty's Stationery Office, London, 1976.
- Newman, J. C., Jr., "Predicting Failure of Specimens with Either Surface Cracks or Corner Cracks at Holes," NASA TN D-8244, June 1976.
- Poe, C. C. Jr., "Stress Intensity Factor for a Cracked Sheet with Riveted and Uniformly Spaced Stringers," NASA TR-T-356, May 1971.
- Bittencourt, T. N., Wawrzynek, P. A., Ingraffea, A. R., and Sousa, J. L., "Quasi-Automatic Simulation of Crack Propagation for 2D LEFM Problems," *Engineering Fracture Mechanics*, Vol. 55, No. 2, 1996, pp. 321–334.
- Swift, T., "Fracture Analysis of Stiffened Structure; Damage Tolerance of Metallic Structures: Analysis Methods and Application," American Society for Testing Materials, ASTM STP 842, 1984, pp. 69–107.
- Dawicke, D. A., Newman, J. C., Jr., Sutton, M. A., and Amstutz, B. E., "Stable Tearing Behavior of a Thin Sheet Material with Multiple Cracks," NASA TM-109131, July 1994.
- Heinimann, M. B., "Analysis of Stiffened Panels with Multiple Site Damage," Ph.D. Dissertation, School of Aeronautics and Astronautics, Purdue Univ., West Lafayette, IN, May 1997.
- Secton, D. G., "A Comparison of Fatigue Damage Resistance and Residual Strength of 2024-T3 and 2524-T3 Panels Containing Multiple Site Damage," M.S. Thesis, School of Aeronautics and Astronautics, Purdue Univ., West Lafayette, IN, May 1997.